Available online at www.sciencedirect.com
ScienceDirect
Surface Science 602 (2008) 416–423
SURFACE SCIENCE
www.elsevier.com/locate/susc

Surface chemistry of acetic acid on clean and oxygen-covered Pd(100)

Zhenjun Li, Feng Gao, W.T. Tysoe *

Department of Chemistry and Biochemistry, Laboratory for Surface Studies, University of Wisconsin-Milwaukee, Milwaukee, WI 53211, USA

Received 14 August 2007; accepted for publication 22 October 2007
Available online 5 November 2007

Abstract

The surface chemistry of acetic acid is studied on clean Pd(100), Pd(100)–p(2 × 2)-O and Pd(100)–c(2 × 2)-O surfaces in ultrahigh vacuum using a combination of temperature-programmed desorption and X-ray photoelectron spectroscopy. The chemistry on clean Pd(100) is similar to that on other palladium surfaces, where molecular acetic acid desorbs at ~200 K and acetate species form at higher temperatures and decompose at ~300 K. In contrast, acetate species predominantly form on the oxygen-covered surfaces and are stable to ~380 K on Pd(100)–p(2 × 2)-O and ~375 K on Pd(100)–c(2 × 2)-O. Acetic acid and its decomposition products, hydrogen, water, carbon monoxide and carbon dioxide form simultaneously at these temperatures.

Keywords: X-ray photoelectron spectroscopy; Temperature-programmed desorption; Acetic acid; Pd(100); Oxygen

1. Introduction

Supported palladium catalyzes the synthesis of vinyl acetate monomer (VAM) from ethylene, acetic acid and oxygen with a selectivity to VAM of ~80%. This is significantly improved by the formation of gold–palladium alloys [1]. The synthesis of vinyl acetate by reaction between ethylene and η^2-acetate species on Pd(111) has been shown to proceed via a pathway first proposed by Samanos et al. [2] where ethylene reacts with adsorbed acetate species to generate an acetoxyethyl–palladium intermediate, which yields VAM through a β-hydride elimination reaction [3]. Goodman et al. used Pd/Au(111) and Pd/Au(100) alloys to study VAM synthesis and discovered that Pd/Au(100) catalyzes the reaction with higher activity than the corresponding (111) surface and identified active ensembles for the reaction that comprise palladium atoms located at the opposite corners of the square unit cell on the (100) face of the alloy, surrounded by gold atoms [4]. This strongly suggests that the catalytic properties of Au/Pd(100) alloys are different from Au/Pd(111) alloys. Catalytic VAM synthesis has also been studied on clean Pd(100) surfaces where the reaction was found to proceed with an activation energy of ~17 kJ/mol and a reaction order in ethylene of −0.4, of acetic acid of 1, and oxygen of 0.5 [5].

Acetic acid adsorbs molecularly on Pd(111) surfaces at low temperatures, forming η^2-acetate species on heating to ~300 K, although the formation of less-stable η^1-species has also been identified spectroscopically [6]. The η^2-acetate species adsorbs with the C–COO plane oriented perpendicularly to the Pd(111) surface with the acetate oxygen atoms located approximately above palladium atop sites [7]. Density functional theory calculations have demonstrated that the acetate species thermally decompose by the C–COO plane tilting such that the methyl group interacts with the surface leading to C—H bond scission [8,9], and the kinetics of this process have been shown to occur explosively, that is, with extremely rapid kinetics, on both carbon-covered Pd(110) [10] and oxygen-covered Pd(111) surfaces [11]. Similar rapid, autocatalytic decomposition of acetic acid has been found on other transition metal surfaces and the origin of this effect discussed in detail [12]. Adsorption of acetic acid on oxygen-covered Pd(111) only slightly increases the extent

* Corresponding author. Tel.: +1 414 229 5222; fax: +1 414 229 5036.
E-mail address: wtt@uwm.edu (W.T. Tysoe).

0039-6028/$ - see front matter © 2007 Elsevier B.V. All rights reserved.
doi:10.1016/j.susc.2007.10.045

of η^2-acetate formation compared to adsorption on the clean surface .

We have recently studied the surface chemistry of ethylene [13] and acetic acid [14] on Au/Pd(1 1 1) alloy surface with various gold compositions where it has been found that the strength of interaction of both molecules increases with increasing palladium content. As a precursor to investigating the surface properties of Au/Pd(1 0 0) alloys, we examine in the following the adsorption and surface chemistry of acetic acid on clean and oxygen-covered Pd(1 0 0) using temperature-programmed desorption and X-ray photoelectron spectroscopy. While this chemistry has been explored on the (1 1 1) and (1 1 0) faces of palladium, surprisingly, no work has, to our knowledge, been carried out on the (1 0 0) face.

2. Experimental

The Pd(1 0 0) substrate (1 cm diameter, 0.5 mm thick) was cleaned using a standard procedure, which consisted of cycles of argon ion bombardment (2 kV, 1 μA/cm^2) and annealing in 4×10^{-8} Torr of O_2 at 1000 K [15]. The cleanliness of the sample was judged using X-ray photoelectron spectroscopy (XPS), Auger electron spectroscopy (AES) and oxygen titrations, where no CO and CO_2 desorb following O_2 adsorption when the sample is carbon free.

Temperature-programmed desorption (TPD) experiments were carried out in an ultrahigh vacuum chamber operating at a base pressure of 8×10^{-11} Torr that has been described in detail elsewhere [16] where desorbing species were detected using a Dycor quadrupole mass spectrometer placed in line of sight of the sample. The sample could be cooled to 80 K by thermal contact to a liquid-nitrogen-filled reservoir and resistively heated to ~1200 K. Temperature-programmed desorption data were collected at a heating rate of 3.6 K/s. The temperature ramp and data collection were controlled using LabView software. This chamber was also equipped with a double-pass cylindrical mirror analyzer for Auger spectroscopy measurements, primarily for monitoring sample cleanliness, and an ion-sputtering gun for sample cleaning.

X-ray photoelectron spectra were collected in a UHV chamber operating at a base pressure of 1×10^{-10} Torr, which was equipped with a Specs X-ray source and a double-pass cylindrical mirror analyzer (CMA) [17]. Spectra were typically collected with a Mg Kα X-ray power of 250 W, at a pass energy of 50 eV. The binding energies were calibrated using the Pd $3d_{5/2}$ feature at 334.8 eV as a standard.

Glacial acetic acid (Aldrich, >99.9% purity) was further purified by means of freeze–pump–thaw cycles and its cleanliness was judged mass spectroscopically. Oxygen (Praxiar, 99.9% purity) was used as received. Both molecules were dosed using capillary dosers that were placed ~1 cm from the front of the Pd(1 0 0) sample to avoid contaminating other parts of the UHV chamber. Note that this arrangement enhances the local pressure close to the sample and an enhancement factor of 100 has been applied to calculate the exposures. Exposures reported in this study are in Langmuirs (1 L = 1×10^{-6} Torr s).

3. Results

3.1. Acetic acid adsorption on Pd(1 0 0)

Temperature-programmed desorption (TPD) is used to monitor desorption and surface reactions of acetic acid. Fig. 1 shows the molecular desorption of acetic acid (60 amu, parent mass) as a function of increasing exposure. At the lowest exposure (0.4 L), one desorption state occurs at ~317 K and a less intense feature appears at ~230 K. With increasing exposure, the 317 K state intensifies, while two more desorption peaks develop at ~247 K and between ~202 and 210 K. The 202–210 K state saturates at an exposure of 1.6 L. Also starting at this exposure, a low-temperature feature develops at 151 K, which grows indefinitely with increasing exposure, suggesting that this is due to multilayer sublimation. A leading-edge plot of ln(Rate) versus $1/T$, shown as an inset to Fig. 1, yields a desorption activation energy of the 151 K state as 48 ± 2 kJ/mol, close to the heat of sublimation of acetic acid. The relative yields of acetic acid in the 202, 247 and

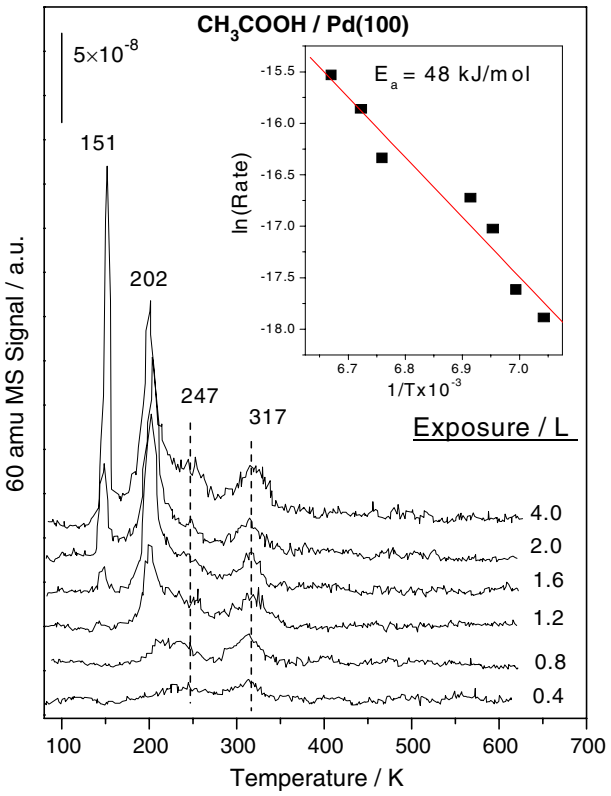

Fig. 1. TPD spectra collected monitoring 60 amu (acetic acid) following adsorption of acetic acid on Pd(1 0 0) at 80 K using a heating rate of 3.6 K/s. Acetic acid exposures (in Langmuir) are given adjacent to the corresponding spectrum.

317 K desorption states measured from the areas under the desorption profiles are 1.0:0.40:0.46.

Fig. 2 displays desorption at 2 (H_2), 18 (H_2O), 28 (CO) and 44 (CO_2) amu at an acetic acid exposure of 3 L, to monitor acetic acid decomposition. Desorption at 60 amu (acetic acid) is also plotted as a reference. Desorption features detected at these masses demonstrate clearly that a portion of chemisorbed acetic acid decomposes to produce H_2O, CO_2, CO and H_2. Note first that the 150 and 203 K features at these masses are assigned to fragmentation of acetic acid. The broad CO_2 desorption peak at 250–550 K indicates that decarboxylation reaction occurs over this temperature range along with the desorption of water (at 18 amu). The 2 amu (H_2) desorption profile shows a broad peak between 290 and 410 K indicating hydrogen is formation-rate limited. Finally, CO desorption is found at ~480 K.

The decomposition of acetic acid on Pd(100) is further monitored using X-ray photoelectron spectroscopy. Fig. 3 shows the C 1s spectral region obtained following the adsorption of 5 L of acetic acid at 80 K and then after annealing to higher temperatures, where the annealing temperatures are displayed adjacent to the corresponding spectrum. The peaks are fitted to Lorentizian profiles, and the peak positions and relative integrated intensities of the features are shown in Table 1. For the as-deposited acetic acid

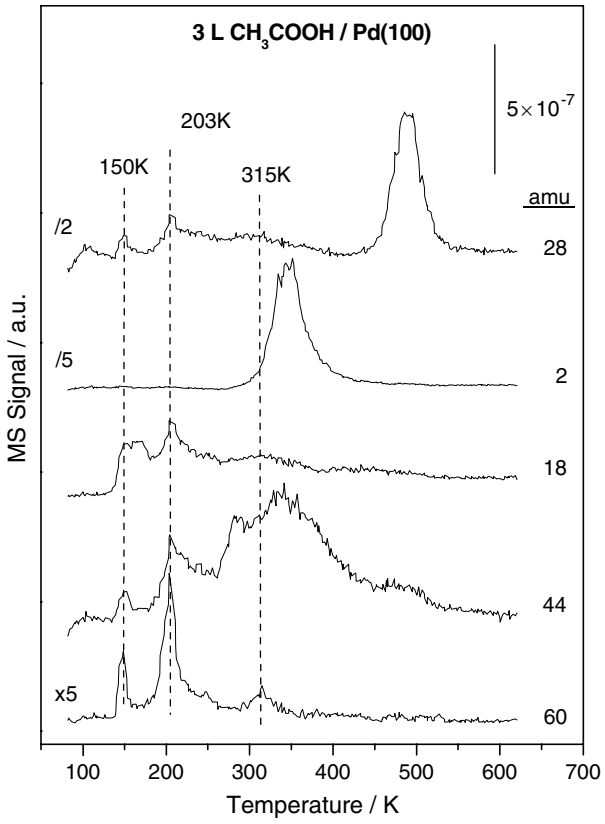

Fig. 2. TPD spectra collected monitoring 2 (H_2), 18 (H_2O), 28 (CO), 44 (CO_2) and 60 (acetic acid) amu following adsorption of 3 L of acetic acid on Pd(100) at 80 K using a heating rate of 3.6 K/s.

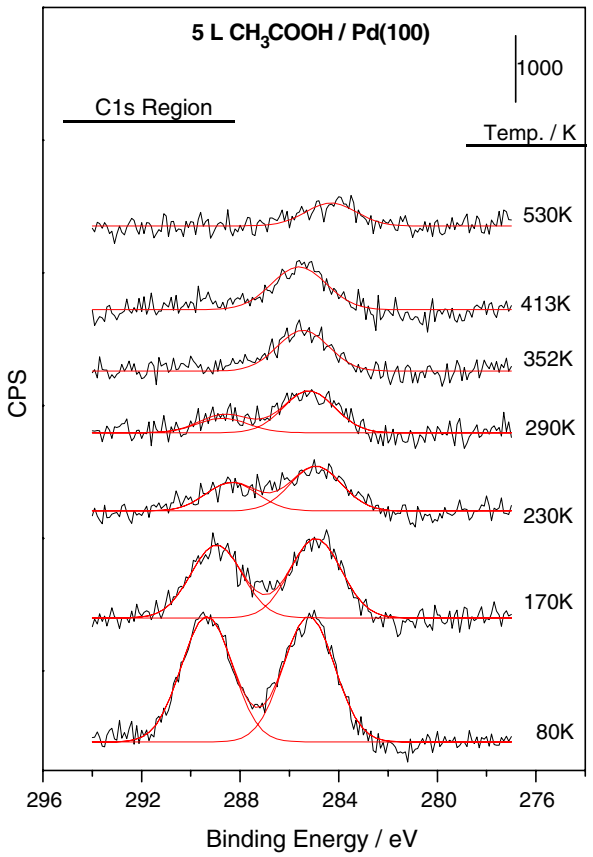

Fig. 3. C 1s photoelectron spectra as a function of annealing temperature adsorption of 5 L of acetic acid on Pd(100) at 80 K. The annealing temperatures are given adjacent to the corresponding spectrum.

Table 1
Binding energies and relative intensities of the C 1s feature obtained following the adsorption of acetic acid on clean Pd(100), taken from Fig. 3

Annealing temperature/K	80	170	230	290
COO C 1s binding energy	285.2	284.9	284.9	285.1
CH_3 C 1s binding energy	289.3	289.0	288.5	288.7
I(COO C 1s)/I(CH_3 C1s)	1.0	1.09	1.57	2.90

Binding energies are within ±0.1 eV.

at 80 K, two well-resolved features are found at 285.2 and 289.3 eV binding energy (BE). The former is assigned to the methyl carbon, and the latter to the carboxylate carbon [6,18,19]. Note that the intensity ratio of these two features is close to unity in agreement with the molecular stoichiometry. After the sample is annealed to 170 K, the intensities of these two peaks decrease due to desorption of the multilayer (Fig. 1), and the binding energies shift to 284.9 and 289.0 eV BE. It should be mentioned that these binding energies agree very well with previous studies of monolayer acetic acid on Pd(111) [6] and Pd(110) [19]. On further warming to 230 K, the intensities of these two peaks continue to decrease and more importantly, the intensity ratio of these two features is no longer unity, where the methyl carbon signal is more intense than that

of carboxylate carbon. Note that this annealing temperature is well below the CO_2 and CO desorption temperatures (Fig. 2) so that the above-mentioned intensity ratio variation is unlikely due to acetic acid decomposition. After annealing the sample to 352 K and above, the carboxylate carbon peak becomes undetectable, leaving a single feature at ~285.5 eV binding energy. This feature persists until 413 K, but disappears on heating to 530 K leaving a single, weak feature at ~284.3 eV BE.

3.2. Acetic acid adsorption on oxygen-covered Pd(100) surfaces

The adsorption of oxygen on Pd(100) has been studied previously [20,21]. It has been found that oxygen dissociatively adsorbs on the surface and forms $p(2\times2)$ islands for coverages in excess of 0.05 ML and yields a fully developed $p(2\times2)$ structure at 1/4 ML coverage at 300 K. The $p(2\times2)$ pattern is then gradually replaced by a $c(2\times2)$ structure as the oxygen coverage increases to 0.5 ML. The sticking coefficient of O_2 on Pd(100) has been found to be constant prior to the full development of the $p(2\times2)$ structure, and to decrease thereafter [22]. Fig. 4a shows the O_2 TPD spectra collected following oxygen adsorption at room temperature as a function of increasing initial exposure. For exposures below 5.2 L, symmetric desorption peaks with desorption peak maxima decreasing with exposure are found, consistent with an expected second-order desorption process. At higher exposures, the desorption peaks become broader due to the development of features at lower temperatures. The corresponding integrated O_2 TPD peak areas are plotted in Fig. 4b as a function of exposure. Fully consistent with previous investigations, it is found that the peak areas increase rapidly with increasing O_2 exposure up to ~5 L, and increase more slowly at higher exposures. Based on this, together with previous studies, it is concluded that a Pd(100)–$p(2\times2)$-O structure forms following a ~5 L O_2 exposure at room temperature. Correspondingly, a Pd(100)–$c(2\times2)$-O superstructure is readily formed by adsorbing ~100 L of O_2 at room temperature. Schematic depictions of these structures are shown in Fig. 4.

The adsorption and reaction of acetic acid is further studied on these two well-defined, oxygen-covered surfaces. Fig. 5 displays molecular acetic acid (60 amu) desorption as a function of exposure following adsorption at 80 K on a Pd(100)–$p(2\times2)$-O surface. At an exposure of 0.4 L, a sharp peak appears at ~382 K, drastically different from desorption from the clean surface (Fig. 1). The intensity of the peak increases with exposure and saturates at an exposure of 1.6 L. At higher exposures, a second desorption feature develops at ~151 K. This feature has the same desorption temperature as for the clean surface, therefore is similarly assigned to multilayer desorption.

Fig. 6 displays a series of TPD spectra from a Pd(100)–$p(2\times2)$-O surface exposed to 3 L acetic acid at 80 K, monitoring desorption of H_2, H_2O, CO and CO_2. Again, desorption at these masses at 151 K is due to fragmentation of desorbing multilayers of acetic acid. Intense signals are detected for 2, 18, 28 and 44 amu at ~382 K (note that

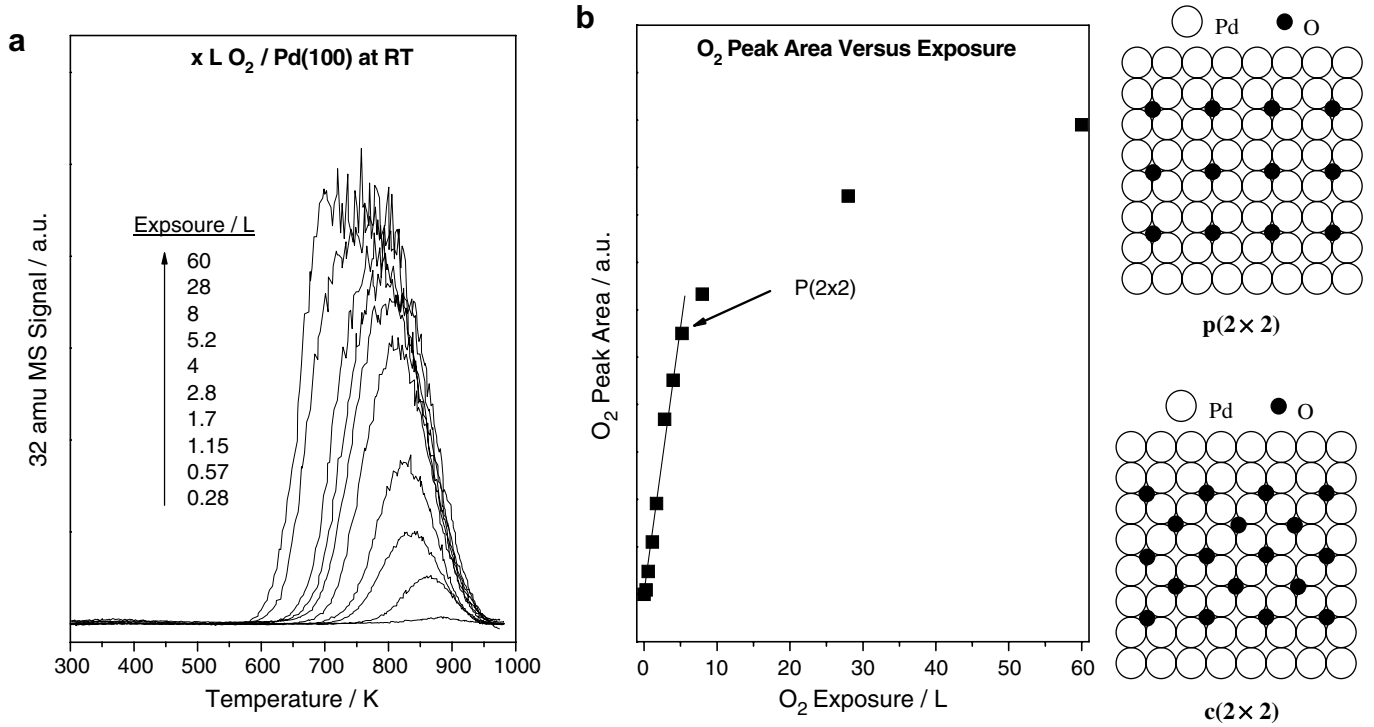

Fig. 4. (a) TPD spectra collected monitoring 32 amu (O_2) following adsorption of O_2 on Pd(100) at room temperature using a heating rate of 3.6 K/s. (b) O_2 peak area as a function of exposure. Shown are schematics of the Pd(100)–$p(2\times2)$-O and Pd(100)–$c(2\times2)$-O structures.

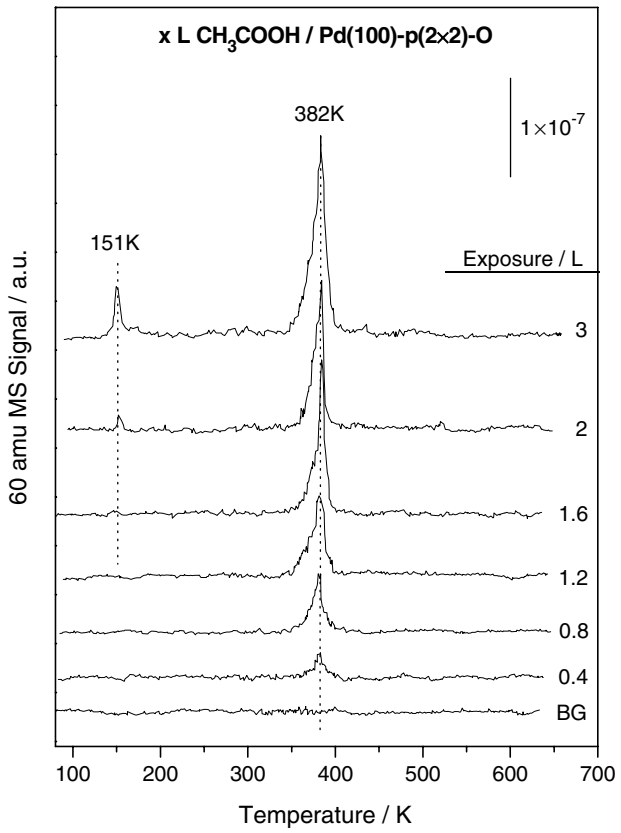

Fig. 5. TPD spectra collected monitoring 60 amu (acetic acid) following adsorption of acetic acid on Pd(100)–p(2 × 2)-O at 80 K using a heating rate of 3.6 K/s. Acetic acid exposures (in Langmuir) are shown adjacent to the corresponding spectrum.

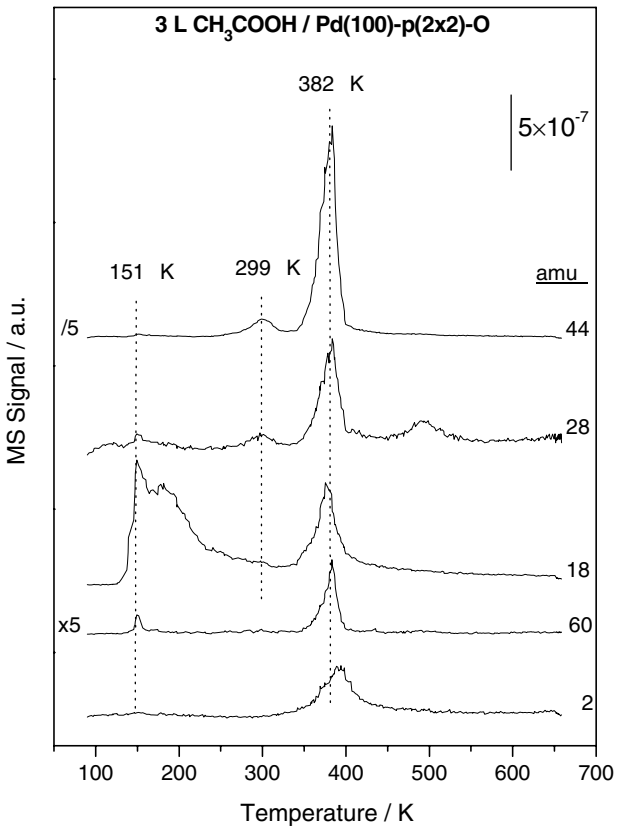

Fig. 6. TPD spectra collected monitoring 2 (H_2), 18 (H_2O), 28 (CO), 44 (CO_2) and 60 (acetic acid) amu following adsorptio of 3 L of acetic acid on Pd(100)–p(2 × 2)-O at 80 K using a heating rate of 3.6 K/s.

44 amu trace is divided by a factor of 5). Although acetic acid indeed desorbs at this temperature (see the 60 amu feature), it is so weak that desorption at other masses cannot merely be fragments of acetic acid and the intense feature at 44 amu suggests that decomposition is the dominating reaction pathway instead. Broad H_2O desorption occurs slightly above 151 K suggesting conversion from acetic acid to acetate starts at about this temperature. Moreover, weak desorption is noticed at 299 K at 18, 28 and 44 amu and a weak CO feature also appears at 480 K.

XP spectra were recorded in order to gain more information regarding acetic acid decomposition on oxygen-covered surfaces. Fig. 7 shows the C 1s region XP spectra following exposure of a Pd(100)–p(2 × 2)-O surface to 5 L acetic acid at 80 K and then annealing to higher temperatures. The as-deposited surface layer displays drastic lineshape differences compared to adsorption on the clean surface (Fig. 3) so that it is no longer possible to fit the features to two peaks. A Lorentzian fit reveals four peaks at 289.8, 288.3, 286.2 and 284.3 eV BE. Note that the 288.3 and 284.3 eV features have a binding energy difference of 4.0 eV, and the 289.8 and 286.2 eV features have a difference of 3.6 eV. Both differences are close to the 4 eV difference for gaseous acetic acid [23], suggesting two distinct species are present. As will be shown below, the lower-binding-energy species is assigned to acetic acid adsorbed onto the surface, and the higher-binding-energy species to multilayer acetic acid (see Table 2). On annealing to 170 K (a temperature where multilayer no longer exists), two features are still detected at 286.7 and 284.0 eV BE, where the lower-binding-energy feature is more intense than the higher-binding energy one; At the same time, there is a satellite peak at 288.7 eV. This feature is also found for acetate on other metal surfaces and explained in term of final state relaxation [24–26]. On further annealing to 248 and 340 K, the spectra are almost identical to that found after annealing to 170 K, suggesting the surface species formed by annealing to this temperature are stable at least to 340 K, consistent with the TPD results (Figs. 5 and 6). Further warming to 420 K and above completely removes surface OCO moieties leaving a small peak at a binding energy of ~285.3 eV, which persists on heating to 490 K. Heating to 580 K leaves a small feature at ~284 eV BE.

Fig. 8 displays desorption at 2 (H_2), 18 (H_2O), 28 (CO), 44 (CO_2) and 60 (acetic acid) amu from a Pd(100)–c(2 × 2)-O surface following exposure to 3 L of acetic acid at 80 K. Again, weak multilayer desorption is noticed at ~151 K. Slightly above this temperature, H_2O (18 amu) desorption is found over a rather wide temperature range and weak H_2O, CO and CO_2 desorption is detected at 293 K. Finally, intense and sharp desorption at all masses monitored is found at 376 K. Finally, Fig. 9 displays the C 1s XP spectra

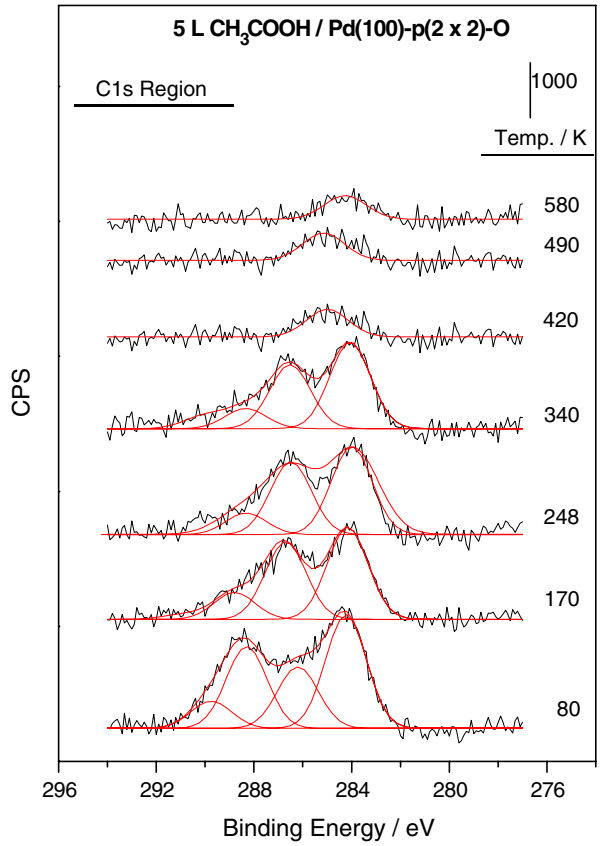

Fig. 7. C 1s photoelectron spectra as a function of annealing temperature adsorption of 5 L of acetic acid on Pd(1 0 0)–p(2 × 2)-O at 80 K. The annealing temperatures are shown adjacent to the corresponding spectrum.

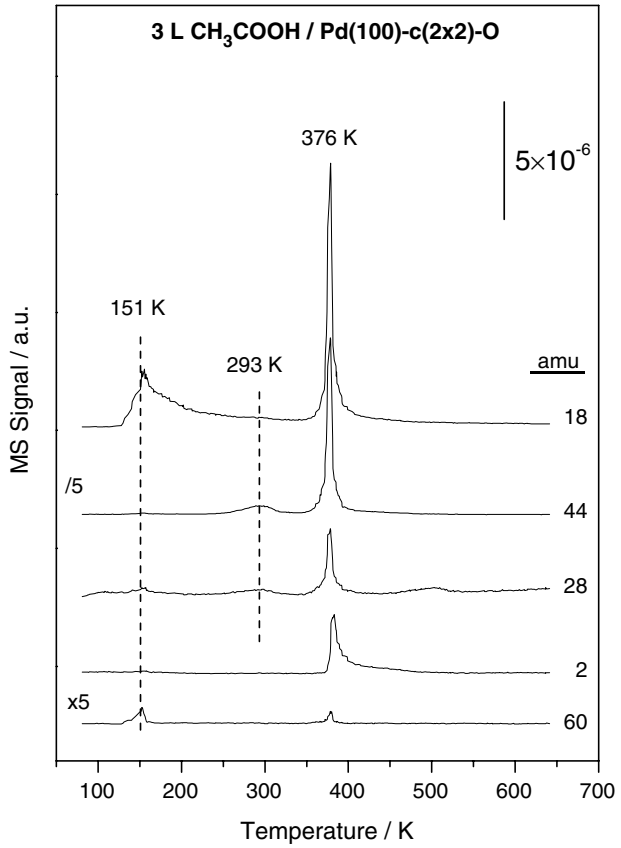

Fig. 8. TPD spectra collected monitoring 2 (H_2), 18 (H_2O), 28 (CO), 44 (CO_2) and 60 (acetic acid) amu following adsorption of 3 L of acetic acid on Pd(1 0 0)–c(2 × 2)-O at 80 K using a heating rate of 3.6 K/s.

Table 2
Binding energies and relative intensities of the C 1s feature obtained following the adsorption of acetic acid on Pd(1 0 0)–p(2 × 2)-O, taken from Fig. 7

Annealing temperature/K	80	170	246	340
COO C1s binding energy	284.2	284.0	284.0	284.0
CH_3 C1s binding energy	288.3	286.7	286.6	286.5
Satellite peak	286.2	288.7	288.4	288.3
I(COO C1*s*)/I(CH_3 C1*s*)	1.39	1.19	1.21	1.35

Binding energies are within ±0.1 eV.

collected following exposure to 5 L of acetic acid to a Pd(1 0 0)–c(2 × 2)-O surface at 80 K, and then annealed to higher temperatures. These spectra resemble those obtained on Pd(1 0 0)–p(2 × 2)-O surfaces (Fig. 7) and will not be described in more detail.

4. Discussion

Acetic acid has been studied on a number single crystal surfaces relevant to this work, including Pd(1 1 1) [6], Pd(1 1 0) [10], and Au/Pd(1 1 1) [13] alloy surfaces with various Au compositions. The study on Pd(1 1 1) reveals that acetic acid adsorbed at 170 K forms two different acetate species as a function of temperature where η^1-acetate species form at 200 K and decompose at 230 K, while η^2-species appear at higher temperatures (>300 K) and decompose at 320 K. Besides decomposition, both species can also rehydrogenate to desorb as acetic acid at similar temperatures at which they decompose, so that the η^1 species hydrogenates to desorb acetic acid at ~230 K and the η^2 species at >300 K on Pd(1 1 1). The TPD data shown in Fig. 1 suggest similar chemistry on Pd(1 0 0). Based on the desorption temperatures for experiments on Pd(1 1 1), we assign the 202 K feature to acetic acid desorption from the monolayer, the 247 K feature to acetic acid formed by hydrogenation of η^1-acetate species and the 317 K feature to acetic acid formed by hydrogenation of η^2-acetate species. These assignments suggest that surface acetate species are generated slightly above 200 K and this is consistent with XPS results shown in Fig. 3.

On the clean surface, the XP spectrum collected following an exposure of 5 L of acetic acid at 80 K reveals two features at 285.2 and 289.3 eV. According to previous investigations [6,18,19], the former is assigned to methyl carbon and the latter to carbon within the –COOH group. On annealing to 170 K, when all multilayer acetic acid has been removed, the C 1s binding energies are found at 284.9 and 289.0 eV, while the ratio of the intensities of these two features is close to unity (see Table 1). Clearly,

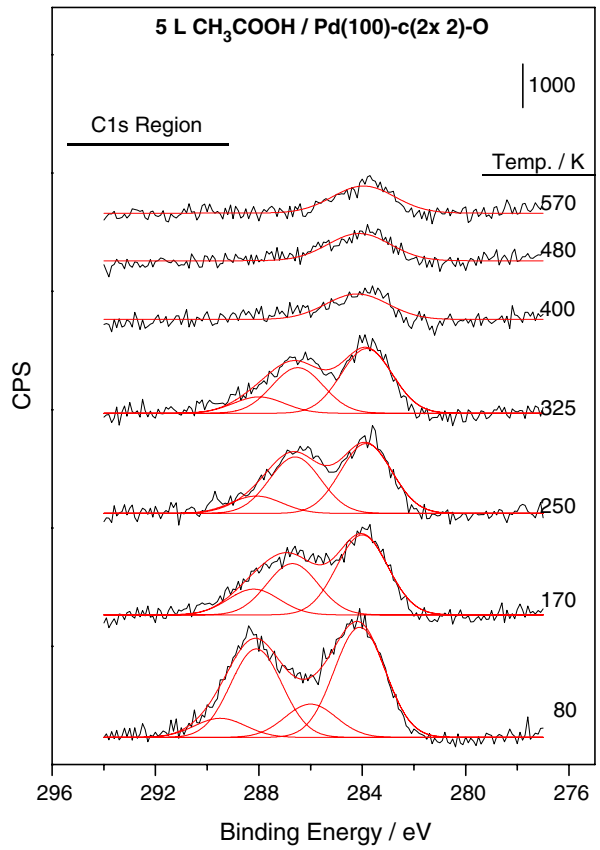

Fig. 9. C 1s photoelectron spectra as a function of annealing temperature adsorption of 5 L of acetic acid on Pd(100)–c(2 × 2)-O at 80 K. The annealing temperatures are shown adjacent to the corresponding spectrum.

features recorded at 80 K contain contributions from both the monolayer and multilayer and the higher binding energies found for the multilayer are consistent with previous studies on Pd(111) [6]. In the case of the multilayer, both the methyl and carboxyl carbons are sampled equally consistent with a relatively randomly oriented film. A larger C 1s intensity for the methyl than the carboxylate carbon has been shown previously to be associated with a C—C bond that is oriented close to perpendicular to the surface indicative of the formation of η^2-acetate species [6,18,19]. Thus, the increased intensity of the methyl C 1s feature on heating to 230 K is consistent with the presence of η^2-acetate species (See Table 1). The desorption profiles shown in Fig. 2, especially the desorption temperatures of various gaseous products, strongly indicate that the majority of H_2O, H_2, CO and CO_2 is formed by decomposition of η^2-acetate species assuming that this gives rise to the 317 K acetic acid desorption state (Fig. 1). The C 1s XPS data (Fig. 3) exhibit a single feature at ~285.5 eV on heating to 352 and 413 K. This binding energy is indicative of the presence of CO on the surface [27]. The feature disappears on heating to 530 K corresponding to the temperature at which carbon monoxide desorbs (Fig. 2) consistent with this interpretation. A weak C 1s feature remains at ~284.3 eV BE after heating to 530 K due to a small amount of carbon remaining on the surface [27].

The surface chemistry on oxygen-covered surfaces is very different from that on the clean surface. Note first that multilayer acetic acid desorbs at the same temperature as from the clean surface, as expected, while rehydrogenation of the acetate species occurs at much higher temperatures (Figs. 5, 6 and 8) indicating a stabilizing role of surface oxygen for acetate species as found previously [11]. The XPS results shown in Figs. 7 and 9 provide direct evidence for the formation of acetate species. First, on a Pd(100)–p(2 × 2)-O surface (Fig. 7), adsorption of 5 L of acetic acid at 80 K reveals a different spectrum compared to its counterpart on the clean surface (Fig. 3). In this case, four peaks at 289.8, 288.4, 286.2 and 284.3 eV BE are found, where the 288.4 and 284.3 eV BE doublet is due to acetic acid adsorbed directly on the surface, while the 289.8 and 286.2 eV BE doublet is due to multilayer adsorption (see Table 2). The spectrum taken at 170 K on the clean surface (Fig. 3) reveals that monolayer acetic acid on clean Pd(100) has corresponding binding energies at 284.9 and 289.0 eV so that first-layer acetic acid on oxygen-covered Pd(100) has binding energy ~0.6 eV lower than on the clean surface. The lower-binding energy of acetic acid on the oxygen-covered surface can be rationalized by postulating less electron transfer from acetic acid to the surface, or alternatively, stronger back donation from the surface to adsorbate when it is precovered by oxygen. As shown in Figs. 6 and 8, spectra taken after annealing to 170 K are very different from those for an acetic acid film annealed to the same temperature on clean Pd(100) (Fig. 3). Especially on both oxygen-covered surfaces, the methyl carbon signal intensity is substantially stronger than the OCO carbon suggesting acetate species are already formed at 170 K. The thermal stability of these species, as verified by both TPD (Figs. 5, 6 and 8) and XPS (Figs. 7 and 9) suggest that these are predominately η^2-acetate species. Note that acetate formation as low as 170 K on oxygen-covered surfaces is consistent with water desorption at low temperatures as shown in Figs. 6 and 8.

It is worth adding a few comments on the autocatalytic decomposition of acetate on oxygen-covered surfaces and this phenomenon has been discussed extensively in the literature [12]. Density functional theory calculations have demonstrated that the acetate species thermally decompose by the C–COO plane tilting such that the methyl group interacts with the surface leading to C—H bond scission [8,9]. Clearly, oxygen adatoms facilitate acetate formation according to the following reaction pathway:

$$2CH_3COOH_{(a)} + O_{(a)} = 2CH_3COO_{(a)} + H_2O$$

If this reaction proceeds ideally and if each acetate species occupies two adjacent Pd atoms, for a Pd(100)–p(2 × 2)-O surface, all oxygen adatoms are removed by forming a saturated acetate overlayer. In contrast, for a Pd(100)–c(2 × 2)-O surface, only half of the oxygen adatoms can be removed. In any case, a close-packed acetate layer will

be formed slightly above 150 K. Clearly, due at least partially to repulsive interactions between acetate species, such acetate layer must be rather thermally stable since the C–COO plane tilting process is not facile. Initial acetate decomposition, perhaps adsorbed at defect sites, will create new sites for other acetate species to decompose in an explosive manner.

5. Conclusions

The surface chemistry on clean Pd(1 0 0) strongly resembles that on other faces of palladium [6,19], where acetic acid desorbs at ~202 K and acetate species form at higher temperatures and thermally decompose at ~300 K to form water, hydrogen, carbon monoxide and carbon dioxide. The major difference between the two surfaces is the effect of oxygen, which on Pd(1 1 1) has little effect on the surface chemistry, in particular the extent of acetate formation, while on Pd(1 0 0), surface oxygen facilitates the formation of acetate species on the surface and stabilizes them so that, on the Pd(1 0 0)–p(2 × 2)-O surface they are stable to above 380 K. This suggests that, on Pd(1 0 0), the oxygen in the vinyl acetate synthesis reaction plays a central role in the formation of active acetate species for the formation of vinyl acetate, while this role is not necessary on Pd(1 1 1).

References

[1] Cat. Gold News, (4) (2003) Spring.
[2] B. Samanos, P. Poutry, R. Montarnal, J. Catal. 23 (1971) 19.
[3] D. Stacchiola, F. Calaza, L. Burkholder, A.W. Schwabacher, M. Neurock, W.T. Tysoe, Angew. Chem. Int. Ed. 44 (2005) 4572.
[4] M.S. Chem, D. Kumar, C.-W. Yi, D.W. Goodman, Science 310 (2005) 291.
[5] D. Kumar, M.S. Chen, D.W. Goodman, Catal. Today 123 (2007) 77.
[6] R.D. Haley, M.S. Tikhov, R.M. Lambert, Catal. Lett. 76 (2001) 125.
[7] J. James, D.K. Saldin, T. Zheng, W.T. Tysoe, D.S. Sholl, Catal. Today 105 (2005) 74.
[8] M. Neurock, J. Catal. 216 (2003) 73.
[9] E. Hansen, M. Neurock, J. Phys. Chem. B 105 (2001) 9218.
[10] M. Bowker, C. Morgan, J. Couves, Surf. Sci. 555 (2004) 145.
[11] J.L. Davis, M. Barteau, Surf. Sci. 256 (1991) 50.
[12] R.J. Madix, J.L. Falconer, A.M. Suszko, Surf. Sci. 54 (1976) 6.
[13] F. Calaza, F. Gao, Z. Li, W.T. Tysoe, Surf. Sci. 601 (2007) 714.
[14] Z. Li, F. Calaza, F. Gao, W.T. Tysoe, Surf. Sci. 601 (2007) 1351.
[15] D. Stacchiola, L. Burkholder, W.T. Tysoe, Surf. Sci. 511 (2002) 215.
[16] Yilin Wang, Feng Gao, W.T. Tysoe, J. Mol. Catal. A—Chem. 236 (2005) 18.
[17] M. Kaltchev, A.W. Thompson, W.T. Tysoe, Surf. Sci. 391 (1997) 14.
[18] M. Bowker, R.J. Madix, Appl. Surf. Sci. 8 (1981) 299.
[19] N. Aas, M. Bowker, J. Chem. Faraday Trans. 89 (1993) 1249.
[20] E.M. Stuve, R.J. Madix, C.R. Brundle, Surf. Sci. 146 (1984) 155.
[21] G. Zheng, E.I. Altman, Surf. Sci. 504 (2002) 253.
[22] G.W. Simmons, Y.-N. Wang, J. Marcos, K. Klier, J. Phys. Chem. 95 (1991) 4522.
[23] S.R. Smith, T.D. Thomas, J. Am. Chem. Soc. 100 (1978) 5459.
[24] M.A. Barteau, R.J. Madix, Surf. Sci. 115 (1982) 355.
[25] J.B. Benziger, R.J. Madix, J. Catal. 65 (1980) 49.
[26] J.C. Fuggle, E. Umbach, D. Menzel, K. Wandelt, C.R. Brundle, Solid State Commun. 27 (1978) 65.
[27] M. Borasio, O. Rodriguez de la Fuente, G. Rupprechter, H.-J. Freunds, J. Phys. Chem. B 109 (2005) 17791.